

Evaluation of the temperature-dependent rheology of non-Brownian particle suspensions via direct numerical simulation

C. R. Leonardi¹, J. W. S. McCullough, D. Wang¹ and S. M. Aminossadati¹

¹School of Mechanical and Mining Engineering
 The University of Queensland, St Lucia, Queensland 4072, Australia

Abstract

This paper presents the recent development and testing of a LBM-DEM model of fluid-particle systems which can predict suspension rheology in the presence of conjugate heat transfer. A total energy formulation of the dual-population thermal lattice Boltzmann method (TLBM) has been extended to include a model of temperature-dependent fluid viscosity. The TLBM-DEM model was then applied to predict the rheology of a range of non-Brownian suspensions in a process referred to as *numerical rheometry*. Isothermal results at high solid volume fractions demonstrated a pronounced increase in relative viscosity. They were also able to highlight the influence of particle friction on suspension behaviour. The inclusion of temperature-dependent fluid viscosity showed a reduced perturbation of the velocity field due to the presence of particles in areas of thinner fluid. Temperature profiles exhibited nonlinearity due to viscous heating stemming from increasing particle solid volume fraction, which increased when conjugate heat transfer was allowed to take place. In the future, this modelling work-flow will be applied to investigate temperature-dependent suspension transport in a number of industrially-relevant flows.

Themes: Computational fluid dynamics; Multiphase and particle-laden flows; Heat transfer.

Introduction

A significant body of research (see [5] for a recent review) has been targeted at the rheological characterisation of non-Brownian suspensions. Despite this, a number of important phenomena are still poorly understood or subject to conjecture. Whilst continuum models are commonly applied to simulate moderately concentrated suspensions, they struggle to capture the nonlinear behaviour that emerges close to maximum packing. In addition, continuum modelling with non-Newtonian and or temperature-dependent fluids is significantly more complicated than the Newtonian case, yet has received little attention in the literature [5]. Complex particle suspensions exist in a range of scientific and engineering contexts, from blood flow to gas production (e.g. hydraulic fracturing fluids), and so improved predictive models of the relevant phenomena are desirable.

Aside from empirical correlations and continuum approximations, computational approaches to model fully-resolved, non-Brownian particle suspensions include Stokesian dynamics [2], smoothed particle hydrodynamics (SPH) [21], and variations of the finite element method [20]. In this work, however, direct numerical simulation of suspensions (i.e. fully resolved modelling) is performed using coupled lattice Boltzmann (LBM) and discrete element (DEM) methods. Since the seminal work of Ladd [8], this approach has been well documented in the literature. Coupled LBM-DEM modelling has the advantage of being able to explicitly and simultaneously capture many relevant phenomena at both the local and global scale, including two-way hydrodynamic coupling [4], non-Newtonian rheology [11], electrostatic [14] and electromagnetic [10] forces.

This paper extends recent work on thermal LBM-DEM suspensions [12, 13] by incorporating a temperature field that facilitates the modelling of conjugate heat transfer and temperature-dependent fluid viscosity. This is then applied to investigate the effective viscosity of suspensions that feature both high solid volume fraction and varying temperature gradients. These results are compared with relevant correlations from the literature. This demonstrates that the modelling approach produces results that are both valid and useful for the investigation of flows that are industrially relevant (e.g. the transport of hydraulic fracturing fluids in unconventional gas reservoirs).

Formulation of the TLBM-DEM Model

The LBM is a *mesoscopic* method that mimics the Navier-Stokes equations at the macroscopic scale. Over that past three decades, it has found wide application in areas such as vehicle aerodynamics, porous media flows, and numerous multiphase and multiphysics problems. The lattice Boltzmann equation,

$$f_i(\mathbf{x} + \mathbf{e}_i \Delta t, t + \Delta t) - f_i(\mathbf{x}, t) = \Omega_i, \quad (1)$$

describes the evolution of a set of particle distribution functions, f_i , via the processes of streaming and collision. The collision term, Ω_i , can take many forms, including variants with single and multiple relaxation times (e.g. BGK, TRT, MRT) and entropic formulations. Both the BGK,

$$\Omega_i^{BGK} = -\frac{\Delta t}{\tau} [f_i(\mathbf{x}, t) - f_i^{eq}(\mathbf{x}, t)], \quad (2)$$

and MRT,

$$\Omega_i^{MRT} = -\mathbf{M}^{-1} \mathbf{S} \mathbf{M} [f_i(\mathbf{x}, t) - f_i^{eq}(\mathbf{x}, t)], \quad (3)$$

collision operators are used interchangeably in this work. In the former, τ is the relaxation parameter, which controls the rate at which f_i approaches its equilibrium value,

$$f_i^{eq} = \omega_i \rho \left[1 + \frac{3}{c^2} (\mathbf{e}_i \cdot \mathbf{u}) + \frac{9}{2c^4} (\mathbf{e}_i \cdot \mathbf{u})^2 - \frac{3}{2c^2} (\mathbf{u} \cdot \mathbf{u}) \right], \quad (4)$$

in which ω_i is a set of lattice-specific weights. In the latter, \mathbf{M} transforms the particle distribution functions to a vector of moments while \mathbf{S} is a diagonal matrix of semi-independent relaxation times. In this work, a two-relaxation-time (TRT) version [6] of the MRT collision operator is employed.

Spatial discretisation is performed using one of either the D3Q15 and D3Q27 lattices. Density, $\rho = \sum_i f_i$, and momentum flux, $\rho \mathbf{u} = \sum_i f_i \mathbf{e}_i$, are calculated as the zeroth and first order moments of f_i , while pressure, $p = c_s^2 \rho$, is evaluated using an equation of state. Here, $c_s = c/\sqrt{3}$ is the fluid speed of sound and $c = \Delta x/\Delta t$ is the lattice speed, where Δx represents the lattice spacing and Δt the explicit LBM time step. Multiscale analysis of the governing equations provides, amongst other things, the relationship between the kinematic viscosity,

$$\nu = \frac{1}{3} \left(\tau - \frac{1}{2} \right) \frac{\Delta x^2}{\Delta t}, \quad (5)$$

the relaxation time, lattice spacing and time step. It is important to note that these equations have been listed in physical units.

To capture the temperature field, the total energy formulation proposed by Guo *et al.* [7] has been implemented along with an expression for temperature-dependent viscosity. In this model the quantity conserved by a second population, g_i , is total energy such that $\sum_i g_i = \rho E$. Here $E = CT + (\mathbf{u} \cdot \mathbf{u})/2$, C is the specific heat of the fluid, and T is the temperature. The complete total energy model incorporates a number of forcing terms that control the collision and relaxation of the respective populations. Only a simplified summary of these is presented here, with the reader referred to the relevant literature [7, 12] for a complete description. In the absence of body forces, the fluid population possess the conventional equilibrium functions and zeroth moment as stated above. In three dimensions, the thermal population possesses an equilibrium of

$$g_i^{eq} = \omega_i p \left[\frac{\mathbf{e}_i \cdot \mathbf{u}}{c_s^2} + \left(\frac{\mathbf{e}_i \cdot \mathbf{u}}{c_s^2} \right)^2 - \frac{\mathbf{u} \cdot \mathbf{u}}{2c_s^2} + \left(\frac{\mathbf{e}_i^2}{2c_s^2} - \frac{3}{2} \right) \right] + E f_i^{eq} \quad (6)$$

which is used with the relaxation equation of,

$$g_i(\mathbf{x} + \mathbf{e}_i \Delta t, t + \Delta t) - g_i(\mathbf{x}, t) = -\tau_g^{-1} (g_i(\mathbf{x}, t) - g_i^{eq}(\mathbf{x}, t)) + \left(1 - (2\tau_g)^{-1} \right) \Delta t q_i + \left(\tau_g^{-1} - \tau^{-1} \right) Z_i \Phi_i. \quad (7)$$

Here $Z_i = \mathbf{e}_i \cdot \mathbf{u} - (\mathbf{u} \cdot \mathbf{u})/2$, $\Phi_i = f_i - f_i^{eq}$ and $q_i = \omega_i \rho E / c_s^2$.

Similarly to viscosity and τ , τ_g is related to the thermal diffusivity of the fluid $\alpha = (\tau_g - 1/2) (\Delta x^2) / (3\Delta t)$. For a fluid with temperature-dependent viscosity, Equation 5 can be used to calculate the required local value of τ based on changing v .

To capture conjugate heat transfer between disparate material phases, the total energy population is used to capture the thermal behaviour of both components. This requires modification of populations crossing material boundaries to ensure that temperature and flux are both conserved (as opposed to total energy, the naturally conserved quantity in this TLBM). The interface condition proposed by Pareschi *et al.* [19] has been implemented here to achieve this.

Particles are modelled as rigid spheres, with their soft-contact interactions and kinematics governed by the discrete element method. Hydrodynamic coupling with the surrounding fluid is enforced with the partially saturated method (PSM) originally proposed by Noble and Torczynski [17]. In this approach, the LBE is modified as,

$$f_i(\mathbf{x} + \mathbf{e}_i \Delta t, t + \Delta t) - f_i(\mathbf{x}, t) = -\mathbf{M}^{-1} \mathbf{S} \mathbf{M} (1 - \beta) \Omega_i^{MRT} + \beta \Omega_i^m, \quad (8)$$

where β is a solid weighting function dependent on the local solid volume fraction, γ , and Ω_i^m is the PSM collision operator. In this work, the superposition PSM collision operator is used,

$$\Omega_i^m = f_i^{eq}(\rho, u_s) - f_i(\mathbf{x}, t) + \left(1 - \frac{\Delta t}{\tau} \right) [f_i(\mathbf{x}, t) - f_i^{eq}(\rho, u)], \quad (9)$$

is applied with a modified solid weighting function [22],

$$\beta = \frac{\gamma \sum_b b (\tau - 1/2)^b}{(1 - \gamma) + \sum_b b (\tau - 1/2)^b}, \quad (10)$$

where $b = 4$ is taken as the summation index. This has been shown [22] to significantly reduce the dependence of hydrodynamic drag on the lattice viscosity (i.e. relaxation parameter).

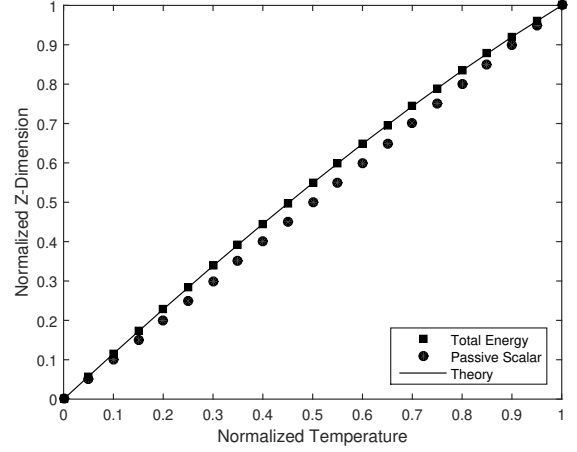


Figure 1: Comparison of temperature profiles computed by total energy and the commonly used passive scalar TLBMs for a Couette flow with temperature-dependent viscosity. Both models generate the non-linear velocity profile accurately.

Modelling of Temperature-Dependent Viscosity

Verification of the developed TLBM model for flows with temperature-dependent viscosity was conducted via comparison to analytical solutions for a Couette flow with an applied temperature gradient. Myers *et al.* [16] presented such solutions for a fluid with viscosity changing through $v = v_0 e^{-\beta T}$ where v_0 is a reference viscosity for $T = 0$ and β is a coefficient controlling the viscosity change. In a normalised form, the velocity profile is given as,

$$u(z) = \sqrt{(2e^{\beta T_m}) / (\beta Br)} \left\{ \tanh \left[z\Theta - \tanh^{-1} \Psi \right] + \Psi \right\}, \quad (11)$$

and the normalized temperature profile by,

$$T(z) = T_m + \beta^{-1} \ln \left\{ 1 - \tanh^2 \left[\tanh^{-1} \Psi - z\Theta \right] \right\}, \quad (12)$$

where $\Theta = \sqrt{(A^2 \beta Br) / (2e^{-\beta T_m})}$ and $\Psi = \sqrt{1 - e^{-\beta T_m}}$. The Brinkman number of the flow is $Br = \mu_0 U_m^2 / k \Delta T$ with k the thermal conductivity of the fluid, U_m the velocity of the moving upper wall (lower wall stationary) and ΔT the temperature change between the walls (upper wall hotter). The terms T_m and A are typically found numerically through application of the boundary conditions at the upper wall at $z = 1$. In an example of $Br = 0.7$ and $\beta = 1.0$, Figure 1 highlights that the current total energy model is required to adequately capture the analytical temperature profile. The commonly used passive scalar approach for TLBM (see e.g. [12]) is not able to resolve this, however both approaches capture the velocity profile accurately.

Numerical Rheometry in a Periodic Shear Cell

A periodic shear cell rheometer was used to compare the isothermal LBM-DEM model to empirical expressions [15, 1, 9] for suspension viscosity. The model domain was periodic in the lateral x - and y -directions. Discrete element platens were mapped to the z -boundaries, with the upper driven by either a constant shear force or velocity and the lower kept static. In this investigation, the rheometer was built with a height of 10 nominal particle diameters. The particle size distribution featured a mean radius of $100 \mu\text{m}$ and a standard deviation of $10 \mu\text{m}$. The

models were run under both stress (15 Nm^{-2}) and strain rate (150 s^{-1}) control. At the end of each simulation, the viscosity ratio, η_r , was calculated as the quotient of the suspension, η_{eff} , and carrier fluid viscosities, η_f . Figure 2 plots the results generated under stress control, showing good agreement with the included empirical expressions. A particularly good match was found with the model of Morris & Boulay [15] up to a dense solid volume fraction of 55% ($\phi \approx 0.55$). Results ob-

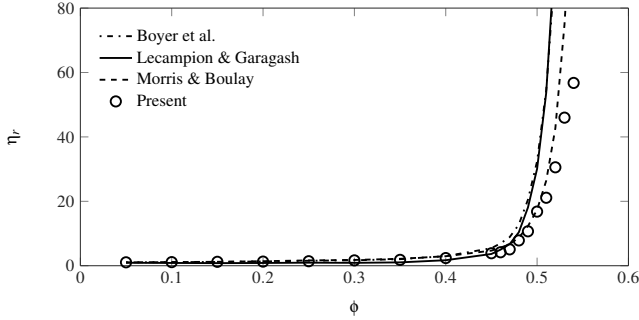


Figure 2: Isothermal viscosity ratio against solid volume fraction when shear under a constant stress.

tained under strain rate control are plotted in Figure 3. With a DEM friction coefficient of 0.1 for the top platen, good agreement with the experimental results of Boyer *et al.* [1] was achieved for $\phi < 0.4$. However, the results deviated dramatically at higher solid volume fractions. This was addressed by increasing the driving platen's friction coefficient to 0.5, mimicking the textured platen (steel bars were attached to the top surface of the rheometer) used in the experiments. This resulted in good agreement up to $\phi \approx 0.65$, which is a result that is rarely seen in the literature. Relative viscosity tests were also conducted

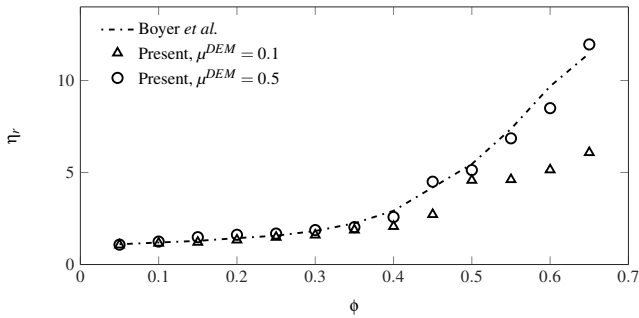


Figure 3: Isothermal viscosity ratio against solid volume fraction, highlighting the influence of friction coefficient.

with and without a fluid possessing temperature-dependent viscosity. Figure 4 compares these outcomes: “TLBM 1” is at $T = 0$ with $v_{LBM} = 1/6$, whilst “TLBM 2” thins according to $v_{LBM} = e^{-T}/6$, $T = 1$ is prescribed for the entire domain. These are compared to three common correlations from the literature [3, 18, 15]. In the “TLBM 2” case, particle motion is less inhibited by the fluid. This results in a greater apparent viscosity of the suspension, especially with increasing solid volume fraction. The general trends observed in the presented results are consistent with the correlations. A shear cell model where the upper and lower platens move at fixed velocities in opposite directions was also been studied. Again, a fluid with temperature-dependent viscosity was considered with the upper wall held at $T = 1$ and the lower wall at $T = 0$. Figure 5 shows that as ϕ increases from 0% to 37%, the non-linearity of both the velocity and temperature profiles increases. The perturbation of

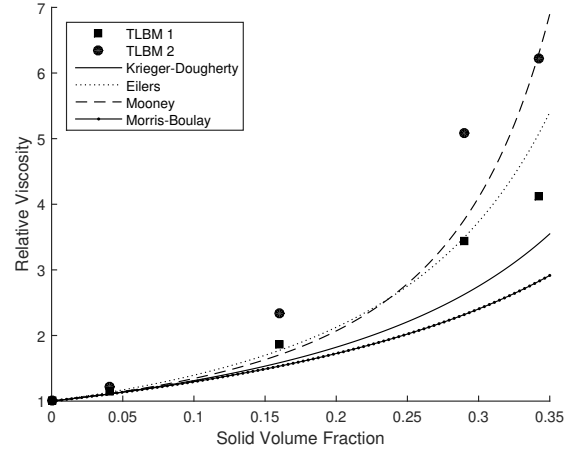


Figure 4: Relative viscosity of suspensions with increasing solid volume fractions. The “TLBM 2” result is for a fluid with temperature-dependent viscosity ($\beta = 1.0$ and $v_{0,LBM} = 1/6$) and a dimensionless temperature of $T = 1$. The lines represent various isothermal correlations.

the velocity profile is reduced in the area of thinner fluid where the flow is less disturbed by the particles. Minor viscous heating caused the change in temperature profile. In Figure 6, conjugate heat transfer has been allowed to occur by reducing the thermal conductivity and specific heat of the solid phase by a factor of three as compared to the fluid. Here the velocity profiles remain largely unchanged but the viscous heating effect can be seen to increase due to this reduction.

Conclusions

A TLBM-DEM model has been developed and applied to predict the effective viscosity of non-Brownian suspensions in the presence of high solid volume fraction, temperature-dependent viscosity, and conjugate heat transfer. It was shown that a total energy formulation of the TLBM is necessary to capture the temperature field in the presence of varying viscosity. Numerical rheometry results were in good agreement with some existing correlations, while appearing to invalidate others. Looking forward, the transport of similar suspensions will be investigated in complex flow configurations, such as hydraulic fracture networks in unconventional gas reservoirs.

References

- [1] Boyer, F. and Minjeaud, S., Numerical schemes for a three component Cahn-Hilliard model, *M2AN*, **45**, 2011, 697.
- [2] Brady, J. and Bossis, G., Stokesian dynamics, *Annu. Rev. Fluid Mech.*, **20**, 1988, 111–157.
- [3] Clausen, J. R., Reasor, D. A. and Aidun, C. K., The rheology and microstructure of concentrated non-colloidal suspensions of deformable capsules, *J. Fluid Mech.*, **685**, 2011, 202–234.
- [4] Cook, B. K., Noble, D. R. and Williams, J. R., A direct simulation method for particle-fluid systems, *Eng. Comput.*, **21**, 2004, 151–168.
- [5] Denn, M. M. and Morris, J. F., Rheology of non-Brownian suspensions, *Annu. Rev. Chem. Biomol. Eng.*, **5**, 2014, 203–228, pMID: 24655134.

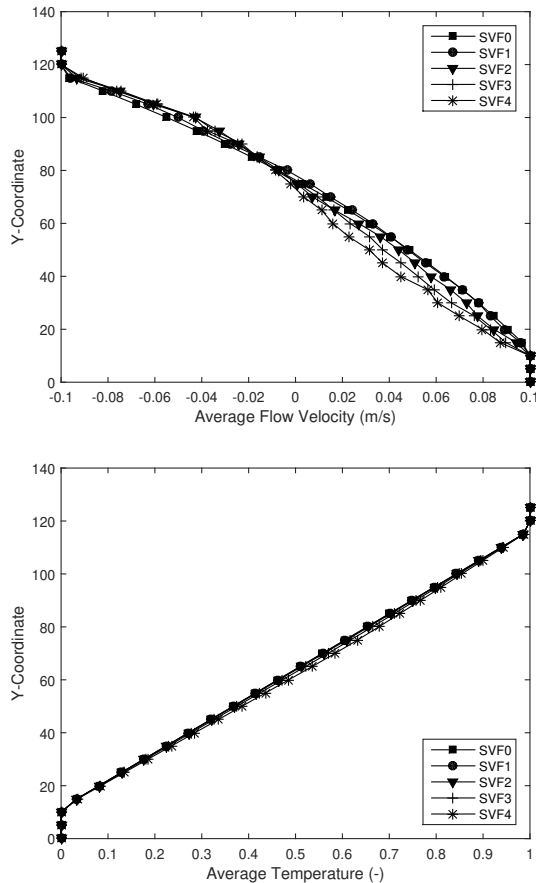


Figure 5: Velocity (upper) and temperature (lower) profiles generated with increasing ϕ , constant strain rate, and temperature-dependent viscosity. Non-linearity can be observed in both.

[6] Ginzburg, I., Verhaeghe, F. and d’Humières, D., Study of simple hydrodynamic solutions with the two-relaxation-times lattice Boltzmann scheme, *Commun. Comput. Phys.*, **3**, 2008, 519–581.

[7] Guo, Z., Zheng, C., Shi, B. and Zhao, T. S., Thermal lattice Boltzmann equation for low Mach number flows: Decoupling model, *Phys. Rev. E*, **75**, 2007, 036704.

[8] Ladd, A. J. C., Numerical simulations of particulate suspensions via a discretized Boltzmann equation. Part 1. Theoretical foundation, *J. Fluid Mech.*, **271**, 1994, 285–309.

[9] Lecampion, B. and Garagash, D. I., Confined flow of suspensions modelled by a frictional rheology, *J. Fluid Mech.*, **759**, 2014, 197–235.

[10] Leonardi, C., McCullough, J., Jones, B. and Williams, J., Electromagnetic excitation of particle suspensions in hydraulic fractures using a coupled lattice Boltzmann-discrete element model, *Comput. Particle Mech.*, 1–16.

[11] Leonardi, C., Owen, D. and Feng, Y., Numerical rheometry of bulk materials using a power law fluid and the lattice Boltzmann method, *J. Non-Newtonian Fluid Mech.*, **166**, 2011, 628–638.

[12] McCullough, J., Leonardi, C., Jones, B., Aminossadati, S. and Williams, J., Lattice Boltzmann methods for the

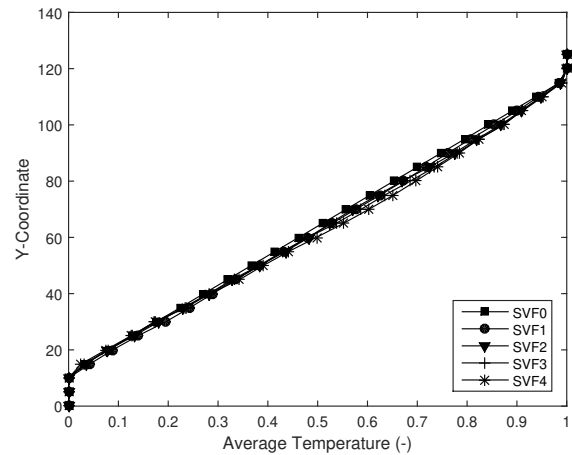


Figure 6: Temperature profile generated with increasing ϕ , constant strain rate, temperature-dependent viscosity, and conjugate heat transfer.

simulation of heat transfer in particle suspensions, *Int. J. Heat Fluid Flow*, **62**, 2016, 150–165.

[13] McCullough, J., Leonardi, C., Jones, B., Aminossadati, S. and Williams, J., Investigation of local and non-local lattice Boltzmann models for transient heat transfer between non-stationary, disparate media, *Comput. Math. Appl.*, **In press**.

[14] Mitchell, T. R. and Leonardi, C. R., Micromechanical investigation of fines liberation and transport during coal seam dewatering, *J. Nat. Gas Sci. Eng.*, **35**, 2016, 1101–1120.

[15] Morris, J. F. and Boulay, F., Curvilinear flows of noncolloidal suspensions: The role of normal stresses, *J. Rheol.*, **43**, 1999, 1213–1237.

[16] Myers, T., Charpin, J. and Tshehla, M., The flow of a variable viscosity fluid between parallel plates with shear heating, *Appl. Math. Modell.*, **30**, 2006, 799–815.

[17] Noble, D. R. and Torczynski, J. R., A lattice-Boltzmann method for partially saturated computational cells, *Int. J. Mod. Phys. C*, **9**, 1998, 1189–1201.

[18] Pal, R., Rheology of suspensions of solid particles in power-law fluids, *Can. J. Chem. Eng.*, **93**, 2015, 166–173.

[19] Pareschi, G., Frapolli, N., Chikatamarla, S. S. and Karlin, I. V., Conjugate heat transfer with the entropic lattice Boltzmann method, *Phys. Rev. E*, **94**, 2016, 013305.

[20] Thogersen, K. and Dabrowski, M., Mixing of the fluid phase in slowly sheared particle suspensions of cylinders, *J. Fluid Mech.*, **818**, 2017, 807–837.

[21] Vazquez-Quesada, A., Bian, X. and Ellero, M., Three-dimensional simulations of dilute and concentrated suspensions using smoothed particle hydrodynamics, *Comput. Particle Mech.*, **3**, 2016, 167–178.

[22] Wang, D., Leonardi, C. R. and Aminossadati, S. M., Improved coupling of time integration and hydrodynamic interaction in particle suspensions using the lattice Boltzmann and discrete element methods, *Comput. Math. Appl.*, **75**, 2018, 2593–2606.